# ABSOLUTELY UNSTABLE WAVES IN INVISCID HYDROELASTIC SYSTEMS

E. DE LANGRE

*Département de Mécanique, Laboratoire d'Hydrodynamique, Ecole Polytechnique-CNRS,*
*91128 Palaiseau, France. E-mail: delangre@ladhyx.polytechnique.fr*

The effect of inviscid plug flow on the stability of several hydroelastic systems is investigated by determining the absolute or convective nature of the instability from the linear dispersion relation. The fluid-structure systems consist of plates and membranes with bounded and unbounded flow. A method is proposed to derive systematically in parameter space the boundary between convective and absolute instability, based on the particular symmetries of the dispersion relation as originally noted by Crighton and Oswell. This method is then applied to the case of plates with superimposed tension, thick plates with rotary inertia and walls made of plates or membranes bounding channel flow, oscillating in a sinuous or varicose mode of deformation. A relation is drawn with solutions by previous authors for plates, for pipes and for the Kelvin–Helmholtz instability with surface tension. To illustrate these results some temporal evolutions are calculated by using an integration in the wavenumber space. Based on the large set of new cases solved in the paper some general trends are discussed as to the influence of flow velocity, confinement and structural stiffness on the existence of absolutely unstable waves in inviscid hydroelastic systems.

© 2002 Published by Elsevier Science Ltd.

## 1. INTRODUCTION

Flexible structures submitted to flow may vibrate for various reasons including turbulence-induced forces, vortex shedding or flutter [1–4]. Practical evidence of the latter case is found in phenomena such as snoring, collapse of blood vessels, flutter of airborne panels or the instability of fluid conveying pipes. Most of the models of such systems have addressed the case where the vibrating structure is of finite length in the direction of flow, and the onset of instability has been tracked from the evolution of the free vibration modes as flow rate is gradually increased. Results of important engineering applicability have been derived; see for instance, references [1–4].

A more local approach considers the conditions for the stability of elastic waves that develop in an elastic structure unbounded in the streamwise direction. Plates, membranes, shells and pipes in confined or unconfined flows have been considered in the literature [5–9]. A further step in that direction is to single out among unstable waves those that are absolutely unstable, i.e. that are not washed away by the flow but eventually contaminate the whole domain. In the general case rather complex effects have been found which involve couplings between the flow instability and the structural instability, see references [10–13]. Considering inviscid uniform flow yields much simpler systems and allows one to derive analytically the dispersion relation. Under this assumption, absolute instability has been

analyzed in generic situations of plates [10, 14–20], membranes [15, 21], shells [17] and pipes [22–24].

In all these cases, it has been observed that the flow velocity promotes absolute instability. Conversely, tension of the structure or foundation stiffness seems to delay such transitions [17, 19, 20, 23, 24]. Flow confinement apparently plays a complex role, much dependent on the nature of the structural stiffness [25, 26]. While absolute instability is not likely to occur in plates as soon as a small curvature stiffens it [17], or in fluid-conveying pipes [24], most systems with a tension rigidity have been found to be absolutely unstable as soon as they become unstable [21, 24, 26].

The goal of the present paper is to systematically determine in parameter space the regions of absolute instability of a variety of structures unbounded in the stream-wise direction under inviscid uniform plug flow. The relation between the above-mentioned situations is also sought to clarify some apparent contradictions or differences. The long-range objective is to shed some light on the global dynamics of the systems of finite lengths starting from their local behaviour, as in references [27, 28]. Though dissipative effects are known to play a role in those instability mechanisms we disregard them in the present analysis.

Consider a slender elastic structure of infinite length in the $x$ direction supporting linear travelling waves so that the local displacement vector is

$$\underline{\xi}(x, y, z, t) = \underline{X}(y, z)e^{i(kx - \omega t)}, \tag{1}$$

where $\underline{X}(y, z)$ denotes the modal shape in the cross-section of the structure. In the absence of fluid, the dynamic equations of the structure yield a linear dispersion relation between the wave number $k$ and the circular frequency $\omega$, which one can write as

$$S(k) - \omega^2 M(k) = 0. \tag{2}$$

where $S$ and $M$ are the stiffness and mass functions respectively. In an appropriate dimensionless form, as will be specified later for each case, this would typically apply to thin plates in bending ($S = k^4$, $M = 1$), thick plates with rotary inertia ($S = k^4$, $M = 1 + k^2$) or membranes ($S = k^2$, $M = 1$). Note that equation (2) applies only to conservative systems, and does not even apply to all of them. Typically, models where the motion of the structure is not reducible to one displacement field, equation (1), cannot be considered simply in this approach, $S$ and $M$ being matrices. This would be the case for high order plate theories and most of shell theories where local displacements and rotations are coupled variables.

In the presence of inviscid plug flow along the axis of the slender structure, the boundary motion modifies the flow velocity into

$$\underline{U} = U\underline{e}_X + \underline{u}, \tag{3}$$

where $U$ is the plug flow velocity and $|u|$ is the perturbation velocity such that $|u| \ll U$. The continuity condition at the boundary $\Sigma$ between the fluid and the structure is [4]

$$\underline{u} \cdot \underline{n} = \left[ \frac{\partial \underline{\xi}}{\partial t} + U \frac{\partial \underline{\xi}}{\partial x} \right] \cdot \underline{n}, \tag{4}$$

where $\underline{n}$ is the normal unit vector at the boundary. We may define a velocity potential $\Phi$ such that $\underline{u} = \underline{\nabla}\Phi$, which is conveniently written as

$$\Phi(x, y, z, t) = -i(\omega - Uk)\phi_k(y, z)e^{i(kx - \omega t)}. \tag{5}$$

The continuity equation $\Delta\Phi = 0$ implies that the reduced potential $\phi_k$ actually depends on the wave number $k$ through

$$\Delta_{yz}\phi_k - k^2\phi_k = 0, \tag{6}$$

where the Laplacian operator $\Delta_{yz}$ refers only to derivatives in the $y$ and $z$ directions. In terms of this potential, the boundary condition (4) is

$$\underline{V}_{yz}\phi_k \cdot \underline{n} = \underline{X} \cdot \underline{n}, \tag{7}$$

where the gradient operator $V_{yz}$ refers only to derivatives in the $y$ and $z$ directions. The resulting pressure is given by the first order terms in the momentum equation

$$p = -\rho\left[\frac{\partial\Phi}{\partial t} + U\frac{\partial\Phi}{\partial x}\right] = \rho(\omega - Uk)^2\phi_k\, e^{i(kx - \omega t)}. \tag{8}$$

The force acting on the slender body projected on the modal shape $\underline{X}$ is

$$f = (\omega - Uk)^2\rho\int_\Sigma (-\phi_k\underline{X} \cdot \underline{n})\, dS. \tag{9}$$

The original dispersion relation for the structure, equation (2), is therefore modified by taking into account the external force due to the presence of the flowing fluid, equation (9). Now, upon introducing a control parameter, say $\varepsilon$, representing a geometrical or mechanical property of the system, it becomes

$$D(\omega, k; U, \varepsilon) = S(k, \varepsilon) - \omega^2 M(k, \varepsilon) - M_A(k, \varepsilon)(\omega - Uk)^2 = 0, \tag{10}$$

where the added mass function has been defined by

$$M_A = \rho\int_{\partial\Omega} (-\phi_k\underline{X} \cdot \underline{n})\, dS. \tag{11}$$

Typical geometries that are considered in this paper have the following dimensionless added mass function: $M_A = 1/|k|$ for a fluid domain of infinite extent as in reference [16], $M_A = 1/(k\tanh k)$ or $M_A = k/\tanh k$ for a domain of finite width [8, 24]. Equation (10) is the general dispersion relation that we consider from now on.

The temporal evolution of a spatially harmonic wave of real wave number $k$ is characterized by the frequencies which are solutions of (10), namely

$$\omega_\pm = \frac{UkM_A \pm [S(M + M_A) - U^2k^2MM_A]^{1/2}}{M + M_A}. \tag{12}$$

The condition of stability of the wave is that the imaginary part of $\omega$ is negative or zero so that

$$S(M + M_A) - U^2k2MM_A \geqslant 0 \tag{13}$$

for all real wave numbers $k$. The critical velocity that brings about instability therefore is

$$U_C(\varepsilon) = \text{Min}_{(k\,real)}\left[\frac{S(k)(M(k) + M_A(k))}{k^2M(k)M_A(k)}\right]^{1/2}. \tag{14}$$

Beyond this flow velocity waves of wavenumber $k$ such that inequality (13) is violated grow with time while others remain neutrally stable.

To further characterize this instability, let us consider the long time behaviour of the impulse response $G(x, t)$ of the system, following reference [29]. The developing instability is said to be *convective* when the wavepacket generated by the impulse is ultimately convected away from the source so that $\lim_{t \to \infty} |G(0, t)| = 0$. Conversely, the instability is said to be *absolute* when the growing wavepacket contaminates the entire domain, upstream and downstream so that $\lim_{t \to \infty} |G(0, t)| = \infty$. In practice, the convective or absolute nature of the instability may be derived directly from the analysis of the dispersion relation (10) without calculating explicitly $G(0, t)$ [30]. It is needed only to consider the absolute frequency and wavenumber, $\omega_0$ and $k_0$ implicitly defined by

$$D(\omega_0, k_0) = 0 \quad \text{and} \quad \frac{\partial D}{\partial k}(\omega_0, k_0) = 0, \tag{15}$$

the absolute or convective nature of the instability being determined by the sign of the imaginary part $\mathrm{Im}(\omega_0)$. It is said to be absolute if $\mathrm{Im}(\omega_0) > 0$ and convective if $\mathrm{Im}(\omega_0) \leqslant 0$. In fact, this criterion is not precise enough as it stands and must be confirmed by a branch analysis in the complex $k$-plane: the root $(\omega_0, k_0)$ must be associated, as $\mathrm{Im}(\omega)$ decreases from large positive values, with pinching of two branches of the dispersion relation $k^+(\omega)$ and $k^-(\omega)$ that originate respectively in the upper and lower halves of the complex $k$-planes [30].

Our aim is to determine for various systems the value of the flow velocity where the instability, if any, shifts from being convective to absolute or *vice versa*. This will be referred to as the transition velocity, $U_T$, which depends on the control parameter $\varepsilon$. Because of the symmetries of the dispersion relations pertaining to different structures in the presence of uniform plug flow, previous authors [16, 17, 19, 23, 31] have pointed out that transition takes place at the triple root of the dispersion relation,

$$D(\omega_T, k_T; \ U_T, \varepsilon) = \frac{\partial D}{\partial k}(\omega_T, k_T; \ U_T, \varepsilon) = \frac{\partial^2 D}{\partial k^2}(\omega_T, k_T; \ U_T, \varepsilon) = 0, \tag{16}$$

and that the corresponding wavenumber $k_T$ is real. This common feature is related to the symmetries in space and time of the dispersion relation for the structure, equation (2), and to the inviscid nature of the flow, yielding in all cases the $(\omega - Uk)^2$ factor. Note that equation (16) is also of interest in the range of stability to derive the transition between evanescent and neutral set of waves [28].

In the general case, the transition velocity $U_T$ may not be explicitly calculated from equation (16). In the next section, we propose a systematic procedure to derive the transition curve $U_T(\varepsilon)$ in parameter space. We then apply it to a large variety of hydroelastic systems. The results are used to explore the effect of different physical parameters on the onset of absolute instability.

## 2. METHODOLOGY

Though the transition velocity $U_T(\varepsilon)$ may not generally be derived explicitly from equation (16), it may, in some cases of polynomial dispersion relations, be obtained as an implicit relationship between $U_T$ and $\varepsilon$ when $k_T$ is varied, see reference [19]. This is generalized here to a much wider set of problems by considering a change of variables from

$(\omega, k, U, \varepsilon)$ to $(\Omega, K, V, \eta)$ such that the dispersion relation reduces to the convenient form

$$\mathbf{D}(\Omega, K; V, \eta) = R(K) - \Omega^2 - \eta F(K)(\Omega - VK)^2 = 0. \tag{17}$$

Provided that $\partial k / \partial K \neq 0$ the transition equation (16) still is in terms of $\mathbf{D}$

$$\mathbf{D}(\Omega_T, K_t; V_T, \eta) = \frac{\partial \mathbf{D}}{\partial K}(\Omega_T, K_t; V_T, \eta) = \frac{\partial^2 \mathbf{D}}{\partial K^2}(\Omega_T, K_t; V_T, \eta) = 0. \tag{18}$$

Upon using the particular form of $\mathbf{D}$ and of its derivatives, one may give after some algebra a parametric definition of $V_T$, $\eta$ and $\Omega_T$ as $K_T$ is varied on the real axis,

$$V_T^2(K_T) = \frac{R - \varphi^2 \psi F}{(\varphi + K_T)^2}, \quad \eta(K_T) = \frac{\psi}{V_T^2}, \quad \Omega_T(K_T) = (\varphi + K_T) V_T \tag{19}$$

with $\varphi = (-b - \sqrt{b^2 - ac})/a$; $\psi = R'/(F'\varphi^2 - 2\varphi F)$; $a = R''F' - R'F''$; $b = 2R'F' - S''F$; $c = -2R'F$, where $(\ )'$ refers to the derivative with respect to $K$. This allows one to define implicitly the relation between the transition velocity $U_T$, and the physical parameter $\varepsilon$. It should be noted here that this solution based on equation (16) allows one to derive the transition curve in the $(U_T, \varepsilon)$ plane, but does not determine which side of this curve is associated with absolute instability (see also reference [31]). This would require the calculation of the absolute frequency at some particular location, with the adequate branch analysis in the complex $k$-plane. In the next sections we take advantage of the results given by other authors for some particular cases to determine the side of the transition curve where absolute instability prevails.

The transition velocity $U_T$ should also be compared with the critical velocity for instability $U_C(\varepsilon)$ defined by equation (14). In terms of the new set of variables this critical velocity may also be given parametrically as a function of the real critical wavenumber $K_C$ as

$$V_C(K_C) = \left[\frac{R^2 F'}{R(F'K_C^2 + 2FK_C) - R'FK_C^2}\right]^{1/2}, \eta(K_C) = \frac{R}{(V^2 K_C^2 - R)F}. \tag{20}$$

## 3  PLATES AND MEMBRANES

The uniform flow of an inviscid incompressible fluid above a flat plate with bending rigidity, Figure 1(a), has been considered by Brazier-Smith and Scott [14], Carpenter and
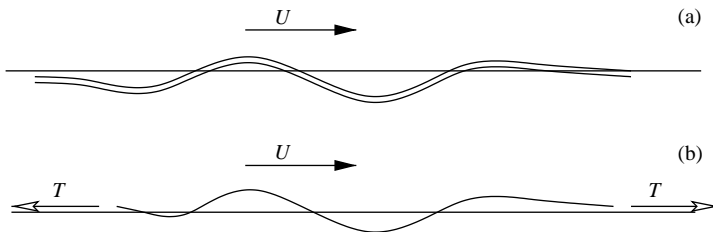


Figure 1. Uniform flow on a flexible surface: (a) plate model; (b) membrane model.

Garrad [15], Crighton and Oswell [16] and Abrahams and Wickham [18]. The corresponding dispersion relation is

$$Bk^4 - m\omega^2 - \rho \frac{1}{|k|}(\omega - Uk)^2 = 0, \tag{21}$$

where $B$ and $m$ are, respectively, the bending stiffness and the mass per unit surface of the plate, $\rho$ and $U$ being the fluid density and flow velocity. Upon using the dimensionless variables $\tilde{U} = Um^{3/2}/\rho B^{1/2}$, $\tilde{k} = km/\rho$ and $\tilde{\omega} = \omega m^{5/2}/\rho^2 B^{1/2}$, it becomes

$$\tilde{k}^4 - \tilde{\omega}^2 - \frac{1}{|\tilde{k}|}(\tilde{\omega} - \tilde{U}\tilde{k})^2 = 0. \tag{22}$$

Instability appears at the onset of flow velocity, $\tilde{U}_C = 0$ and a transition from convective to absolute instability is found [14–16] at

$$\tilde{U}_T = \left[\frac{2^2 5^5}{3^3}\left(2 - \frac{15^{1/2}}{2}\right)\right]^{1/4} \simeq 0{\cdot}074. \tag{23}$$

A similar but simpler problem has been considered by Kelbert and Sazonov [21], with a tension-induced rigidity ("membrane" model) instead of the bending rigidity ("plate" model), Figure 1(b). The corresponding dispersion relation is

$$Tk^2 - m\omega^2 - \rho \frac{1}{|k|}(\omega - Uk)^2 = 0, \tag{24}$$

where $T$ is the tension applied in the plane of the membrane. Upon using new dimensionless variables pertaining to tension, $\bar{U} = Um^{1/2}/T^{1/2}$, $\bar{k} = km/\rho$ and $\bar{\omega} = \omega m^{3/2}/\rho T^{1/2}$, it becomes

$$\bar{k}^2 - \bar{\omega}^2 - \frac{1}{|\bar{k}|}(\bar{\omega} - \bar{U}\bar{k})^2 = 0. \tag{25}$$

As the flow velocity is increased instability sets in at $\bar{U}_C = 1$, and it is convective up to the value of

$$\bar{U}_T = (6\sqrt{3} - 9)^{1/2} \simeq 1{\cdot}18, \tag{26}$$

where it becomes absolute [21].

Using the methodology proposed in the present paper, one may now study the gradual transition from a stiff plate, equation (23), to a tensioned membrane, equation (26), by considering a plate with superimposed tension, the ratio between the corresponding rigidities being varied. The dispersion relation combining bending and tension rigidities is

$$Bk^4 + Tk^2 - m\omega^2 - \rho \frac{1}{|k|}(\omega - Uk)^2 = 0. \tag{27}$$

and is, in the dimensionless variables pertaining to bending,

$$\tilde{k}^4 + \tilde{T}\tilde{k}^2 - \tilde{\omega}^2 - \frac{1}{|\tilde{k}|}(\tilde{\omega} - \tilde{U}\tilde{k})^2 = 0, \tag{28}$$

where the dimensionless tension $\tilde{T} = m^2 T/\rho^2 B$ scales the ratio between rigidity induced by tension and that from bending. Upon introducing $\Omega = \tilde{T}^2 \tilde{\omega}$, $K = \tilde{T}\tilde{k}$, $V = \tilde{T}\tilde{U}$, $\eta = \tilde{T}$ the dispersion relation becomes

$$\mathbf{D}(\Omega, K; V, \eta) = K^4 + K^2 - \Omega^2 - \eta \frac{1}{|K|} (\Omega - VK)^2 = 0. \tag{29}$$

It displays the convenient form of equation (17), with $R(K) = K^4 + K^2$ and $F(K) = 1/|K|$. Upon using equation (19) the computation of the transition velocity $\tilde{V}_T$ versus the parameter $\eta$ is straightforward, and the effect of tension and velocity on the nature of the instability may be derived. For the sake of clarity, one can here use the combined dimensionless velocity

$$U^* = \frac{U}{\sqrt{(T/m) + (\rho^2 B/m^3)}} = \frac{\tilde{U}}{\sqrt{\tilde{T} + 1}} = \frac{\bar{U}}{\sqrt{1 + 1/\tilde{T}}} . \tag{30}$$

such that, for small tensions, $\tilde{T} \ll 1$, one has $U^* \simeq \tilde{U}$, and for large tensions $\tilde{T} \gg 1$, $U^* \simeq \bar{U}$. In terms of this velocity, the stability diagram is shown in Figure 2, including the instability threshold given by equation (14). At the low values of the tension parameter, the solution of Crighton for a plate [16] is obtained, with a very low instability threshold $\tilde{U}_C \simeq 0$ and absolute instability arising at $\tilde{U} \simeq 0.074$. Conversely, for high tensions the solution of Kelbert [21] for pure membranes is obtained, with a critical velocity $\bar{U}_C = 1$ and a transition velocity $\bar{U}_T \simeq 1.18$. These limits allow one to determine the side of the transition curve where absolute instability prevails, here above the curve.
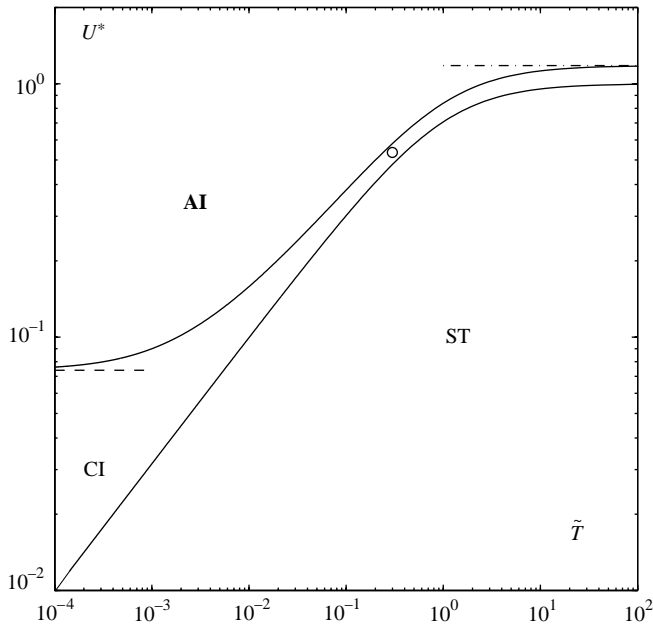


Figure 2. Domains of absolute instability (**AI**), convective instability (CI) and stability (ST) for a plate with superimposed tension. (- - -) Limit of Crighton and Oswell [16] for a plate without tension. (- · - · -) Limit of Kelbert and Sazonov [21] for a pure membrane. (○) Approximate solution of Peake and Sorokin [19] for a sandwich panel case.

The results of Figure 2 show that a small amount of tension is sufficient to modify significantly the propagation of waves on the plate. First, instability appears at non-zero flow velocity. Second, the domain of convective instability is significantly reduced. This may be related to the analysis of Peake [17] regarding the influence of stiffness due to curvature on absolute instability in plates. A very small amount of curvature was found to increase significantly both the critical and the transition velocities. As previously noted [24, 17] the pure plate configuration seems to yield rather pathological results.

Some relation may also be found with the work of Peake and Sorokin [19] on a sandwich panel case. The dispersion relation they consider as a limit case of a more general problem reads, using our variables,

$$\tilde{k}^4 + \tilde{T}\tilde{k}^2 + \alpha - \tilde{\omega}^2 - \frac{1}{|\tilde{k}|}(\tilde{\omega} - \tilde{U}\tilde{k})^2 = 0, \tag{31}$$

and the transition velocity is given in the range of $0 \leqslant \tilde{T} \leqslant 0.3$ while $\alpha = \tilde{T}^2/80$ is found to have a small influence. In Figure 2 the corresponding point with $\tilde{T} = 0.3$ and $U^* \simeq 0.53$ falls near our transition curve.

We consider now the influence of rotary inertia in the plate, using the dispersion relation

$$Bk^4 - Jk^2\omega^2 - m\omega^2 - \rho\frac{1}{|k|}(\omega - Uk)^2 = 0, \tag{32}$$

where $J$ is the rotary inertia of the plate section. In dimensionless form this is

$$\tilde{k}^4 - (1 + \sigma\tilde{k}^2)\tilde{\omega}^2 - \frac{1}{|\tilde{k}|}(\tilde{\omega} - \tilde{U}\tilde{k})^2 = 0, \tag{33}$$

with $\sigma = \rho^2 J/m^3$. A fully consistent model for a thick plate should include the effect of shear deformation (see reference [32, 33]). The dispersion relation would then contain a term $\omega^4$ which may not be taken into account easily in the present approach. It should nevertheless be noted that for a plate of uniform density $\rho_s$ and thickness $h$ the dimensionless inertia $\sigma$ scales as $(\rho/\rho_S)^2$ whereas the coefficient associated with shear deformation scales as $(\rho/\rho_S)^4$. It may be inferred that equation (32) has some relevance for $(\rho/\rho_S) \ll 1$.

Upon using a further transformation $\Omega = \sigma\tilde{\omega}$, $K = \sqrt{\sigma}\tilde{k}$, $V = \sqrt{\sigma}\tilde{U}$, $\eta = \sqrt{\sigma}$, one obtains the generic form

$$\mathbf{D}(\Omega, K; V, \eta) = \frac{K^4}{1 + K^2} - \Omega^2 - \eta\frac{1}{|K|(1 + K^2)}(\Omega - VK)^2 = 0. \tag{34}$$

The domain of absolute instability is readily derived in terms of the rotary inertia parameter $\sigma$ and the flow velocity $\tilde{U}$, see Figure 3. The reduced rotary inertia $\sigma$ is seen to promote absolute instability. This may be analyzed in terms of wave velocity. In the absence of fluid, the phase velocity using equation (32) with $\rho = 0$, is

$$c^2 = \left(\frac{\omega}{k}\right)^2 = \frac{Bk^2}{m + Jk^2}, \tag{35}$$

which has an upper bound $c_\infty = \sqrt{B/J}$. In Figure 3 it appears that for $\sigma \gg 1$ absolute instability sets in as soon as
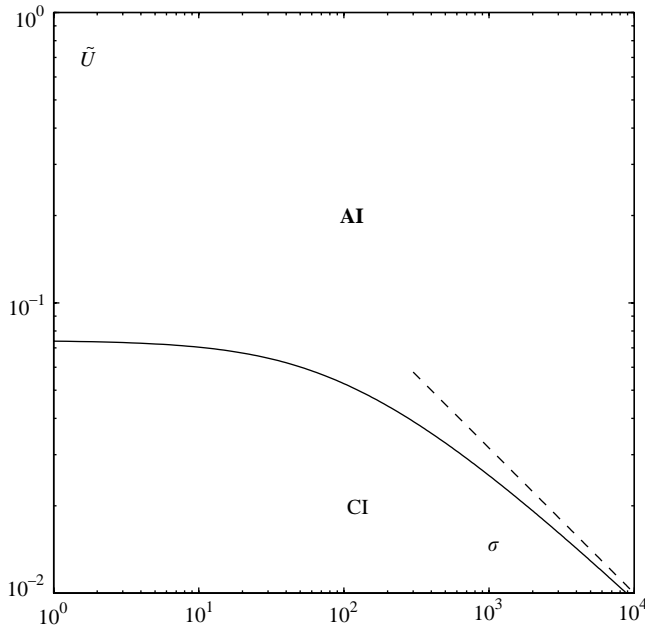
$$\tilde{U} > 1/\sqrt{\sigma}, \tag{36}$$

Figure 3. Domain of absolute instability (**AI**) for a plate with rotary inertia. (- - -) Upper limit of phase velocity in the plate without fluid, equation (36).

which in dimensional variables is $U > c_\infty$. In that particular case, absolute instability arises when the flow velocity becomes larger than all phase velocities in the plate.

## 4. CHANNEL FLOW

Consider now the case of two identical parallel plates of infinite extent bounding a plane channel of width $2e$. When the two plates are restricted to have the same transverse displacement, they are subjected to a sinuous mode of deformation as opposed to a varicose mode, Figure 4(a), the transverse displacement being governed by the dimensionless dispersion relation [8, 26]

$$\tilde{k}^4 - \tilde{\omega}^2 - \frac{\tanh \tilde{k}\tilde{e}}{\tilde{k}} (\tilde{\omega} - \tilde{U}\tilde{k})^2 = 0, \tag{37}$$

with the dimensionless channel width $\tilde{e} = \rho e / m$. The generic change of variables is now made, where $\Omega = \tilde{e}^2\tilde{\omega}$, $K = \tilde{e}\tilde{k}$, $V = \tilde{e}\tilde{U}$, $\eta = \tilde{e}$ and the dispersion relation becomes

$$\mathbf{D}(\Omega, K; V, \eta) = K^4 - \Omega^2 - \eta \frac{\tanh K}{K} (\Omega - VK)^2 = 0. \tag{38}$$

The transition velocity $V_T$ may be numerically derived. This is now expressed in terms of the dimensionless velocity $\tilde{U}$, Figure 5(a), as a function of the dimensionless channel width, $\tilde{e}$. For asymptotically large channels the transition curve is consistent with the limit value of equation (23) for a plate. This limit allows one to determine which side of the transition curve is the zone of absolute instability, here above the curve.
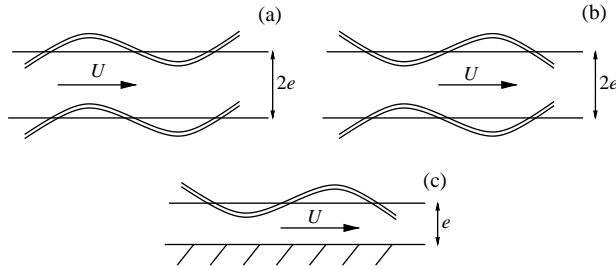
Figure 4. Plates with channel flow. (a) Sinuous deformation of walls in channel flow, (b) varicose deformation of walls in channel flow, (c) rigid wall at a finite distance from the flexible plate.
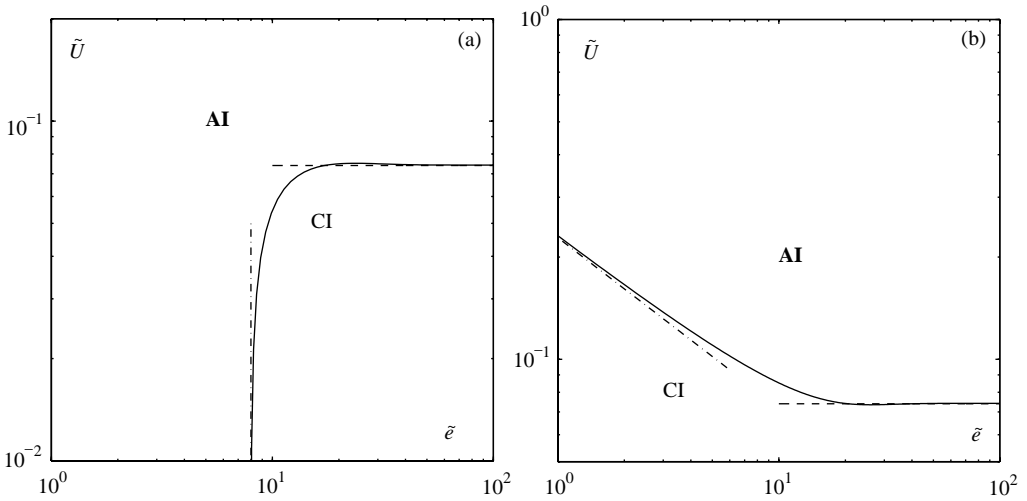


Figure 5. Domain of absolute instability (**AI**) for plates bounding channel flow. (- - -) Single plate with unbounded fluid domain, equation (23) [16]. (a) Sinuous mode, (-.-.-) limit for a thin channel, $\tilde{e} = 8$, [24], (b) varicose mode, (-.-.-) limit for a thin channel, equation (42).

The limit $\tilde{e} = 8$ observed in Figure 5(a) may be understood by considering a long wavelength approximation in equation (37), namely $\lambda = 2\pi/k \gg e$. In that limit one has $\tilde{k}\tilde{e} \ll 1$ so that $\tanh \tilde{k}\tilde{e} \simeq \tilde{k}\tilde{e}$ and the dispersion relation reduces to

$$\tilde{k}^4 - \tilde{\omega}^2 - \tilde{e}(\tilde{\omega} - \tilde{U}\tilde{k})^2 = 0. \tag{39}$$

This is identical in form with the dispersion relation for beam-like motions of a fluid-conveying pipe, see reference [1–4]. In that case, [22, 24], the transition between absolute and convective instability takes place at a dimensionless mass ratio $\beta = \tilde{e}/(\tilde{e} + 1) = 8/9$, i.e., $\tilde{e} = 8$.

The case of opposite displacement of the two plates, i.e., that of varicose modes Figure 4(b), yields a similar dimensionless dispersion relation

$$\tilde{k}^4 - \tilde{\omega}^2 - \frac{1}{\tilde{k}\tanh \tilde{k}\tilde{e}}(\tilde{\omega} - \tilde{U}\tilde{k})^2 = 0. \tag{40}$$

This also applies to the case of a rigid wall at a distance $e$ from the flexible plate, Figure 4(c). Upon using the same variables $V$, $K$, $\Omega$ and $\eta$ and the same procedure as above, but now

with $F(K) = 1/(K \tanh K)$, the transition curve may also be derived, Figure 5(b), see also reference [26]. Again the limit case $\tilde{U} = 0.074$ is obtained in the limit of large channels and allows one to define the side of the transition boundary where absolute instability prevails. For channels of very small width, equation (40) reduces to

$$\tilde{k}^4 - \tilde{\omega}^2 - \frac{1}{\tilde{e}\tilde{k}^2}(\tilde{\omega} - \tilde{U}\tilde{k})^2 = 0, \tag{41}$$

and the direct use of criterion (16) gives the exact transition velocity:

$$\tilde{U} = \frac{2^{1/2}3^2}{5^{5/2}}\frac{1}{\sqrt{\tilde{e}}} \simeq \frac{0.228}{\sqrt{\tilde{e}}}. \tag{42}$$

When plotted in Figure 5(b), this limit is found to be consistent with our results for the more general case. It should be noted that Walsh [8] observed that the particular value of $\sqrt{\tilde{e}}\,\tilde{U} = 0.228$ caused a "coalescence of roots" in this system. Figure 5 shows that the solution of Crighton and Oswell [16] for the infinite plate applies only to very large channels, typically $\tilde{e} > 10$, that is in terms of dimensional parameters $\rho e > 10$ m. Combining Figures 5(a) and 5(b) shows that plates bounding channel flow undergo absolute instability through the sinuous mode of deformation first.

Let us now consider similar channels with walls made of membranes instead of plates. For a sinuous mode of deformation the linear dimensionless dispersion relation is

$$\bar{k}^2 - \bar{\omega}^2 - \frac{\tanh \bar{k}\bar{e}}{\bar{k}}(\bar{\omega} - \bar{U}\bar{k})^2 = 0, \tag{43}$$

with $\bar{e} = \rho e/m$. In this particular case of membranes where $R(K) = K^2$ the critical velocity may not be derived by using the parametric definition of equation (20), which provides only the limit value $\bar{U}_C = 1$ for $\bar{e} \to \infty$. With the use of the original definition of the critical velocity, equation (14), one has here

$$\bar{U}_C = \left(\frac{1 + \bar{e}}{\bar{e}}\right)^{1/2}. \tag{44}$$

With a further change of variables $\Omega = \bar{e}\bar{\omega}$, $K = \bar{e}\bar{k}$, $V = \bar{U}$, $\eta = \bar{e}$, the generic form of the dispersion relation becomes

$$\mathbf{D}(\Omega, K; V, \eta) = K^2 - \Omega^2 - \eta\frac{\tanh K}{K}(\Omega - VK)^2 = 0 \tag{45}$$

and the transition velocity may be plotted in terms of the channel width, see Figure 6(a).

Here the particular solution of Kelbert and Sazonov [21], equation (26), is obtained for wide channels $\bar{e} \gg 1$. This proves that the domain of absolute instability stands above the transition curve. The particular case of small width $\bar{e} \ll 1$ is directly obtained from the transition relation as

$$\bar{U}_T = 1/\sqrt{\bar{e}}. \tag{46}$$

In this limit the waves are not dispersive and there is no relevance in using the concept of absolute instability. These results are fully consistent with those obtained in reference [24] for a tensioned pipe conveying fluid.
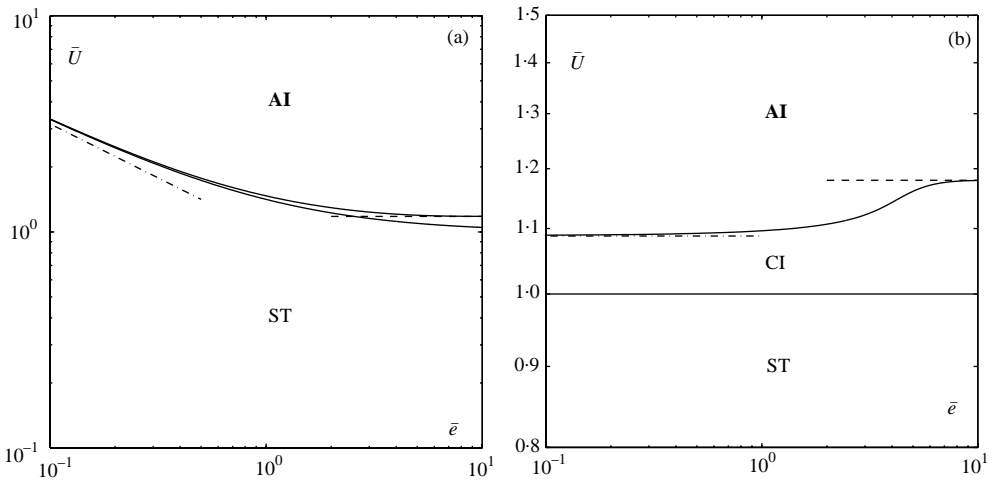
Figure 6. Domain of absolute instability (**AI**) for membranes bounding channel flow. (- - -) Single membrane with unbounded fluid domain, equation (26) [21]. (a) Sinuous mode, (-·-··-) limit for thin channel, equation (46), [24], (b) varicose mode, (-·-··-) limit for thin channel, equation (49).

As far as varicose modes are concerned, instability arises at the critical velocity $\bar{U}_C = 1$ and the reduced dispersion relation becomes

$$\mathbf{D}(\Omega, K; V, \eta) = K^2 - \Omega^2 - \eta \, \frac{1}{K \tanh K} \, (\Omega - VK)^2 = 0. \tag{47}$$

The transition curve is given in Figure 6(b), see also reference [26]. Again, the limit for wide channels is consistent with the solution of Kelbert and Sazonov [21]. In the limit of small channel width the dispersion relation is

$$\bar{k}^2 - \bar{\omega}^2 - \frac{1}{\bar{e}\bar{k}^2} (\bar{\omega} - \bar{U}\bar{k})^2 = 0 \tag{48}$$

and the transition velocity may be explicitly calculated as

$$\bar{U}_T = \frac{2^{5/2}}{3^{3/2}} \simeq 1 \cdot 09. \tag{49}$$

This particular value is also found here as the lower limit of the general case, Figure 6(b). Combining Figures 6(a) and 6(b) shows that membranes bounding channel flow undergo absolute instability through the varicose mode of deformation first, in contrast with walls made of plates.

## 5. RELATION WITH THE KELVIN-HELMHOLTZ INSTABILITY

Let us now analyze unstable waves propagating in a membrane bounded by two fluids, Figure 7, with a plug flow of velocity $U$ and density $\rho_1$ on one side and still fluid with density $\rho_2$ on the other side. The dispersion relation is similar to equation (24) with a new
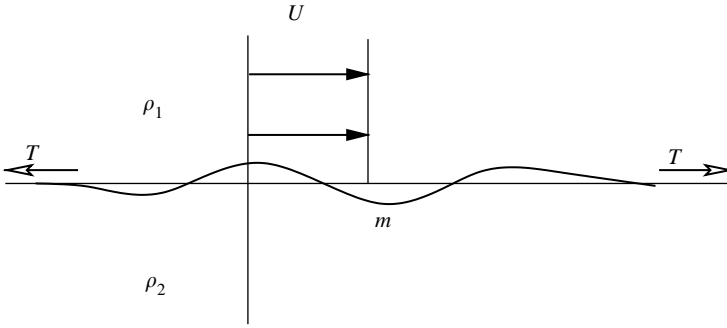
Figure 7. Kelvin–Helmholtz instability with a membrane at the interface between the two fluids.

inertia term associated with the still fluid domain, namely

$$Tk^2 - \left(m + \rho_2 \frac{1}{|k|}\right)\omega^2 - \rho_1 \frac{1}{|k|}(\omega - Uk)^2 = 0. \tag{50}$$

The particular case of a massless membrane, $m = 0$, models the Kelvin–Helmholtz instability with surface tension [34, 31]. Conversely with $\rho_2 = 0$ one can model the case of uniform flow along a flexible membrane, as discussed in the preceding sections. We now seek to relate these two extreme cases by varying the mass ratio in the system.

Using the dimensionless variables pertaining to tension with $\rho_1$ as the reference density we have

$$\bar{k}^2 - \left(1 + \frac{\chi}{|\bar{k}|}\right)\bar{\omega}^2 - \frac{1}{|\bar{k}|}(\bar{\omega} - \bar{U}\bar{k})^2 = 0, \tag{51}$$

where $\chi = \rho_2/\rho_1$ is the mass ratio between the two fluids. Note that here no gravity effects are considered. The critical velocity as given by equation (14) is here

$$\bar{U}_C = \text{Min}_{\bar{k}} \left[\frac{\bar{k}^2 + \bar{k}(1 + \chi)}{\bar{k} + \chi}\right]^{1/2}. \tag{52}$$

It abruptly varies from $\bar{U}_C = 1$ for $\chi = 0$ (uniform flow over a flexible membrane) to $\bar{U}_C = 0$ as soon as a domain of still fluid exists, $\chi > 0$. The dispersion relation is now transformed into

$$\mathbf{D}(\Omega, K; V, \eta) = \frac{|K|K^2}{1 + |K|} - \Omega^2 - \eta \frac{1}{1 + |K|}(\Omega - VK)^2 = 0, \tag{53}$$

upon using the particular change of variables $\Omega = \omega/\chi$, $K = \bar{k}/\chi$, $V = \bar{U}$, $\eta = 1/\chi$.

Using again the parametric definition of the transition velocity, one may give its dependence on the mass ratio $\chi$, Figure 8. In the limit of $\chi \ll 1$ where the still fluid vanishes, one obtains the solution of equation (26) for a membrane submitted to a uniform flow. It appears that for $\chi > 1/3$, i.e., $\rho_2 > \rho_1/3$, the instability is always absolute. At the particular value of $\chi = 1$, and without considering any mass at the interface, $m = 0$, Triantafyllou [31] showed that absolute instability sets in as soon as $U > 0$. Our results of Figure 8 yield that absolute instability is found when $U\sqrt{m/T} > 0$, that is when $U > 0$ for any value of $m$ except for the limit case $m = 0$, where the solution of reference [31] applies. This shows full consistency between our results and those of reference [31].
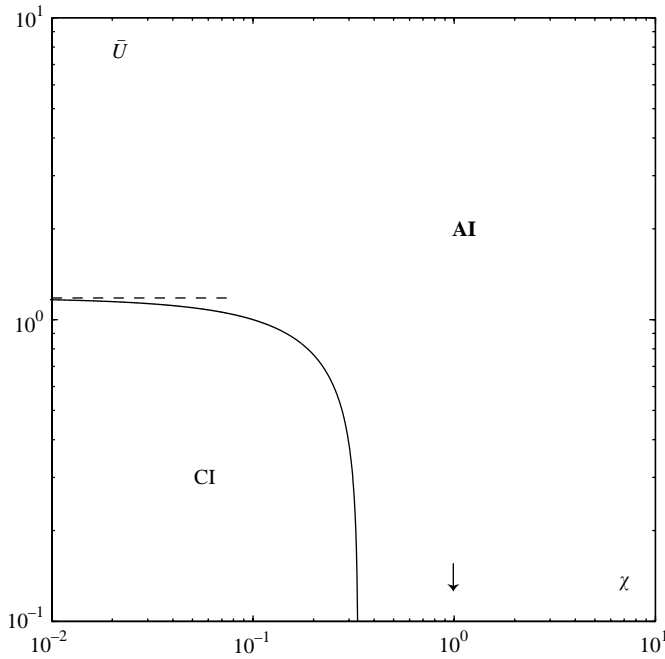
Figure 8. Domain of absolute instability (**AI**) for a membrane separating two different fluids in terms of the mass ratio. (– – –) Equation (26) [21]. (↓) Kelvin–Helmholtz instability with surface tension for two fluids of equal density [31].

## 6. TEMPORAL RESPONSE

In order to illustrate these transitions from convective to absolute instability we may consider the time evolution of the systems described by equation (17) following a particular set of initial condition. Let $y(X, T)$ be any variable of interest in the structure, $X$ and $T$ being the space and time variables associated with $K$ and $\Omega$ for each particular case. With Gaussian initial conditions, i.e., considering the evolution of an initial hump of unit amplitude

$$y(X, 0) = e^{-(X/X_0)^2}; \quad \frac{\partial y}{\partial t}(X, 0) = 0, \tag{54}$$

the temporal evolution is obtained as a Fourier integral

$$y(X, T) = \mathbf{R_E}\left[\int_{-\infty}^{+\infty} (\alpha^+ e^{i(KX - \Omega^+ T)} + \alpha^- e^{i(KX - \Omega^- T)})\,dK\right], \tag{55}$$

where the coefficients $\alpha^+$ and $\alpha^-$ are such the initial conditions (54) are satisfied and where $\Omega^\pm(K)$ are the solutions of the dispersion relation (17). These conditions yield

$$\alpha^\pm = \frac{X_0}{4\sqrt{\pi}}\left[1 \mp \frac{\eta VFK}{\Delta}\right]e^{-(X_0 K/2)^2}; \quad \Omega^\pm = \frac{\eta VFK \pm \Delta}{1 + \eta F}, \tag{56}$$

with $\Delta^2 = R(1 + \eta F) - \eta F V^2 K^2$. This integration with respect to $K$ is valid only if the range of unstable wavenumbers is bounded so that non-causal situations are avoided (see also reference [24]).
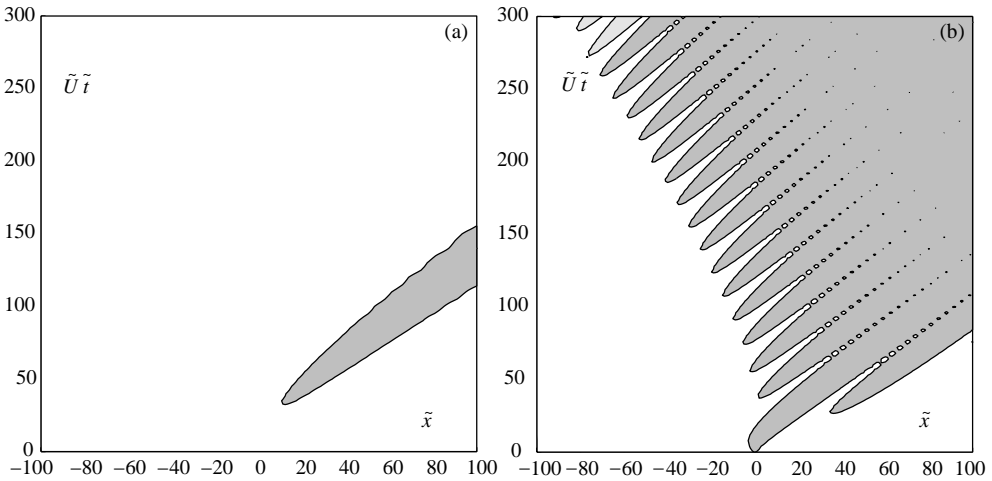
Figure 9. Temporal evolution of plates bounding channel flow to a Gaussian initial condition $y(0, t) = \exp(-\tilde{x}/\tilde{x}_0)^2$ with $\tilde{x} = 10$, moving in a varicose mode of deformation. The gray region is the domain in time–space where the plate displacement exceeds the maximum of the initial condition. (a) Case of convective instability $\tilde{U} = 0.05$, (b) case of absolute instability $\tilde{U} = 0.20$. In both cases $\tilde{e} = 10$.

We apply this procedure to derive the evolution of the channel with walls made of plates, moving in a varicose mode, configuration of equation (40), Figure 5(b). For a set of parameters where the instability is convective ($\tilde{e} = 10$ and $\tilde{U} = 0.05$), Figure 9(a), the domain of the plate where the amplitude exceeds the maximum of the initial condition, $|y| > 1$ is seen to widen while being convected out. Conversely, for larger values of the flow velocity, ($\tilde{e} = 10$ and $\tilde{U} = 0.20$), Figure 9(b), the instability contaminates the upstream part of the plate and it is clearly absolute as predicted.

## 7. EFFECT OF PHYSICAL PARAMETERS ON THE NATURE OF THE INSTABILITY

The effect of the plug flow velocity $U$ on the existence of absolute instabilities has been discussed in the particular case of fluid-conveying pipes in reference [24]. It was noted that flow velocity plays a double role in the dynamics of the system: by advecting perturbations it favours convective instabilities, but its influence on growth rates might lead to absolute instabilities. In all the cases considered in the present paper, as well as those analyzed by previous authors [10, 14–17, 21–24], it appears that the instability always becomes absolute at sufficiently large flow velocity.

The stiffness and mass functions of the structure, $S(k)$ and $M(k)$, have also a strong influence on the nature of unstable waves. In our results a significant difference exists between the effect of a stiffness function of the fourth order in $k$ (plate) and that of the second order (membrane). For plates, Figures 3 and 5, large domains of convective instability are found. For membranes, Figure 6, instability becomes absolute slightly above the critical velocity. These conclusions are in fact opposite to those obtained in the comparison between flexural and tensioned pipes, as discussed in reference [24]. A simple but improper interpretation was then proposed to relate the prevalence of convective instability to bounded phase velocities, found in tensioned pipes. It was then thought that a bounded phase velocity would ultimately be overcome by advection, thereby bringing about convective instability. The new results given in Figure 3 prove that this is not the case: by

introducing a rotary inertia the phase velocity in the plate is bounded but absolute instability is nevertheless found to prevail. In fact, in the limit of large inertia, absolute instability sets in precisely when the flow velocity becomes larger than the phase velocity of waves in the plate.

The effect of added mass is also of crucial importance. In the frame of the inviscid fluid model all forces exerted by the flow are scaled by the added mass function $M_A(k)$. Added mass depends on the wavenumber $k$ and the geometry of the fluid domain through the velocity potential $\phi_k$, equation (11). Consider here the mass ratio

$$\mu(k) = \frac{M_A(k)}{M(k)} \tag{57}$$

which is, for a given wavenumber, the relative proportion between the inertia convected with the flow velocity $M_A(k)$ and the inertia of the structure $M(k)$, including that of the still fluid in the case of the Kelvin–Helmholtz instability. Note that several parameters influence $\mu$: the ratio between the fluid density and that of the structure, the wavenumber, and the confinement, which is the reduction of the cross-section of the fluid domain. The latter parameter is known to increase the added mass. All the results of the preceding sections may be reanalyzed in terms of the mass ratio $\mu$ instead of the geometrical parameters. To do so we shall use the common length scale $\lambda = m/\rho$ and evaluate $\mu$ at the non-dimensional wavenumber $\bar{k} = \tilde{k} = 1$. The results obtained in the preceding section for plates with rotary inertia, and for sinuous and varicose modes of plate walls with channel flow, Figures 3 and 5, are now shown in terms of the mass ratio, Figure 10(a). A good continuity is found between these results which indicates that $\mu$ satisfactorily takes into account the confinement effect. Clearly, increasing the confinement, and therefore the moving mass, promotes convective instability in plates whatever the geometry of the fluid domain. The results of Figure 6 pertaining to wave propagation in membranes with channel flow are also shown, in Figure 10(b), displaying also a good continuity. In that case the mass ratio $\mu$ seems to favour absolute instability in contrast with the case of plates. This may be
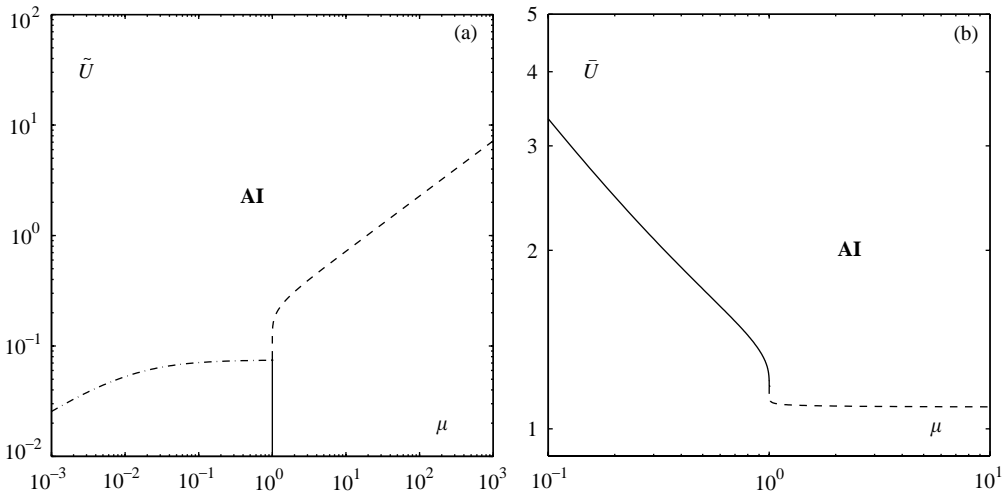


Figure 10. The effect of ratio between moving and non-moving mass on the domain of absolute instability. (a) Plates (-.-) plate with rotary inertia, (- -) channel in a varicose mode of deformation, (——) channel in a sinuous mode of deformation; (b) membranes (- -) channel in a varicose mode of deformation, (——) channel in a sinuous mode of deformation.
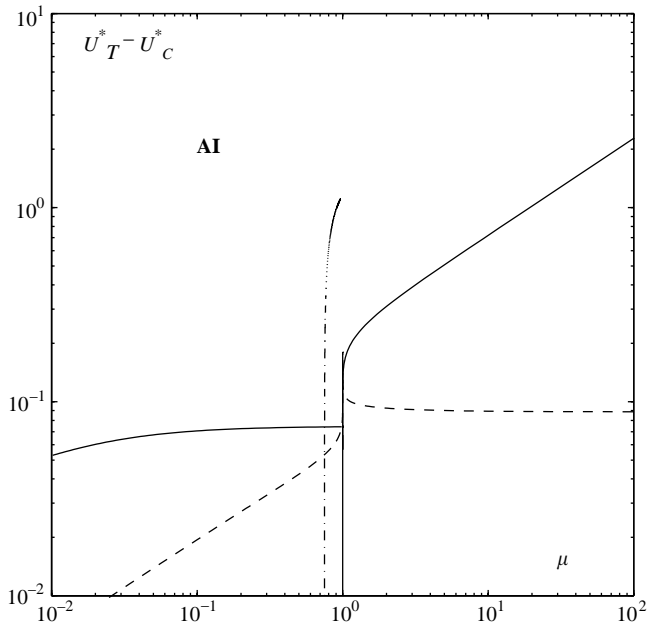
Figure 11. The effect of the ratio between moving and non-moving mass on the domain of absolute instability in all cases considered in the paper. (——) Plates, (- -) membranes, (- . -) Kelvin–Helmholtz instability with a membrane at the interface.

understood by considering that the added mass also plays a role in a negative stiffness term of the dispersion relation namely through $-U^2 M_A k^2$. For membranes where the structural stiffness also varies in $k^2$, this results in a non-zero critical velocity, as found in the preceding sections. In Figure 6, it may be seen that the variation of the transition velocity $U_T$ closely follows the trends of the critical velocity.

We now gather all the results of the present paper on the same graph by plotting the difference between the transition velocity and the critical velocity, namely $U_T^* - U_C^*$, versus the mass ratio $\mu$, Figure 11. All transition curves increase with the mass ratio, so that we may assert that moving mass generally promotes convective instability in inviscid hydroelastic systems.

## 8. CONCLUSION

We have proposed a new method to derive systematically in parameter space the limit between convective and absolute instability for inviscid hydroelastic systems. Through its application to a large set of configurations, gaps have been filled between most solutions derived by previous authors for particular cases of plates, membranes or pipes. In particular, by varying the tension superimposed on a flexible plate we have continuously related the solution given by Crighton and Oswell [16] for a plate to the solution for a membrane given by Kelbert and Sazonov [21]. By varying the width of the fluid domain we have related the plate solution of [16] to the pipe solution by Kulikovskii and Shikina [22], and similarly, the membrane solution in reference [21] to the tensioned pipe solution by de Langre and Ouvrard [24]. The case of varicose modes in a channel or, equivalently, of a flexible boundary near a rigid wall has been fully solved, with closed-form solutions for vanishing channel width.

A relation has also been established between the membrane case [21] and the analysis of Triantafyllou [31] for the Kelvin–Helmholtz instability with surface tension, by continuously varying the mass ratio between the moving and non-moving fluids. The temporal evolution following a Gaussian initial condition has been given to illustrate the results.

Considering all the results derived in the present paper we may now state some general conclusions on the effects of physical parameters on the existence of absolutely unstable waves in inviscid hydroelastic systems. The flow velocity has been shown always to favour absolute instability. Conversely, confinement of flow promotes convective instability through its effect on the ratio between added fluid mass and mass of the solid. Structural stiffness, and more specifically its dependence on wavenumber, plays a crucial role on the instability threshold, but apparently not directly on the transition to absolute instability. Preliminary results using the same method on other systems such as panels of finite width or shells reveal similar trends [35].

The methodology proposed in this paper to derive the limit between convective and absolute instability is much simpler than the systematic branch analysis in the complex $k$-plane used by other authors. In fact, such a branch analysis is still needed at some point to determine which side of the transition curve is the domain of absolute instability. Though our parametric definition of the transition velocity requires that no dissipative effects are taken into account in the hydroelastic model, its simplicity allows one to explore a large variety of systems. It may therefore help understand, in a wider range of applications, the physics of unstable wave propagation in flow-induced vibrations of structures.

The relation between the local behaviour of such waves and the global instabilities that arise in systems of finite extent is explored in reference [28] for the particular case of fluid-conveying pipes.

## REFERENCES

1. R. D. BLEVINS 1991 *Flow-Induced Vibration*. New York: Van Nostrand Reinhold
2. E. NAUDASCHER and D. ROCKWELL 1994 *Flow-Induced Vibrations: an Engineering Guide*. Rotterdam: Balkema.
3. E. H. DOWELL 1995 *A Modern Course in Aeroelasticity*. Dordrecht: Kluwer Academic.
4. M. P. PAÏDOUSSIS 1998 *Fluid-structure Interactions. Slender Structures and Axial Flow*, Vol. 1. London: Academic Press.
5. E. H. DOWELL 1966 *American Institute of Aeronautics and Astronautics Journal* **4**, 1370–1377. Flutter of infinitely long plates and shells. Part I: plates.
6. D. S. WEAVER and M. P. PAÏDOUSSIS 1977 *Journal of Sound and Vibration* **50**, 117–132. On collapse and flutter phenomena in thin tubes conveying fluid.
7. W. ROTH 1964 *Ingenieur-Archiv* **33**, 236–263. Instabilität durchströmter Rohre.
8. C. WALSH 1995 *Journal of Fluids and Structures* **9**, 393–408. Flutter in one-dimensional collapsible tubes.
9. L. HUANG 1998 *Journal of Fluids and Structures* **12**, 131–151. Reversal of the Bernouilli effect and channel flutter.
10. A. LUCEY and P. CARPENTER 1992 *Journal of Fluid Mechanics* **234**, 121–146. A numerical simulation of the interaction of a compliant wall and an inviscid flow.
11. K. S. YEO, B. C. KHOO and H. Z. ZHAO 1999 *Journal of Sound and Vibration* **223**, 379–398. The convective and absolute instability of fluid flow over viscoelastic compliant layers.
12. O. WIPLIER and U. EHRENSTEIN 2000 *Journal of Fluids and Structures* **14**, 157–182. Numerical simulation of linear and non-linear disturbance evolution in boundary layer with compliant walls.
13. O. WIPLIER and U. EHRENSTEIN 2001 *European Journal of Mechanics/B-Fluids* **20**, 127–144. On the absolute instability in a boundary-layer flow with compliant coatings.
14. P. R. BRAZIER-SMITH and J. F. SCOTT 1984 *Wave Motion* **6**, 547–560. Stability of fluid flow in the presence of a compliant surface.

15. P. W. CARPENTER and A. D. GARRAD 1986 *Journal of Fluid Mechanics* **170**, 199–232. The hydrodynamic stability over Kramer-type compliant surfaces. Part 2. Flow-induced surface instabilities.

16. D. CRIGHTON and J. E. OSWELL 1991 *Philosophical Transactions of the Royal Society of London A* **335**, 557–592. Fluid loading with mean flow. I. Response of an elastic plate to localized excitation.

17. N. PEAKE 1997 *Journal of Fluid Mechanics* **338**, 387–410. On the behaviour of a fluid-loaded cylindrical shell with mean flow.

18. I. D. ABRAHAMS and G. R. WICKHAM 2001 *Wave Motion* **33**, 7–23. On transient oscillations of plates in moving fluids.

19. N. PEAKE and S. V. SOROKIN 2001 *Journal of sound and Vibration* **242**, 297–617. On the behaviour of fluid-loaded sandwich panels with mean flow.

20. ZHAO HANGZONG and K. S. YEO 2001 *American Institute of Aeronautics and Astronautics Journal* **39**, 740–742. Absolute instability of a potential flow over a plate-spring system.

21. M. KELBERT and I. SAZONOV 1996 *Pulses and other wave processes in fluids.* Modern Approaches in Geophysics. Dordrecht: Kluwer Academic.

22. A. G. KULIKOVSKII and I. S. SHIKINA 1988 *Izvestia Akademii Nauk Arminskoĭ SSR* **41**, 31–39. On the bending oscillation of a long tube filled with moving fluid.

23. G. S. TRIANTAFYLLOU 1992 *Physics of Fluids A* **4**, 544–552. Physical condition for absolute instability in inviscid hydroelastic coupling.

24. E. DE LANGRE and A. E. OUVRARD 1999 *Journal of Fluids and Structures* **13**, 663–680. Absolute and convective bending instabilities in fluid-conveying pipes.

25. E. DE LANGRE 2000 in *Proceedings of the International Conference on Theoritical and Applied Mechanics, ICTAM2000, Chicago.* TAM Report 580, 66–66, paper GL-08. Absolutely unstable waves in hydroelastic systems.

26. E. DE LANGRE 2000 *Comptes-Rendus à l'Académie des Sciences, Série IIb*, **328**, 61–65. Ondes variqueuses absolument instables dans un canal élastique.

27. O. DOARÉ and E. DE LANGRE 2000 in *Flow-induced Vibrations* (S. Ziada and T. Staubli, editors), 349–354. Rotterdam: Balkema. Local and global instability of fluid-conveying cantilever pipes.

28. O. DOARÉ and E. DE LANGRE 2002 *Journal of Fluids and Structures* **16**, 1–14. Local and global instability of fluid-conveying pipes on elastic foundation.

29. A. BERS 1983 in *Handbook of Plasmas Physics* (M. N. Rosenbluth and R. Z. Sagdeev, editors), Vol 1, 451–517. Amsterdam: North-Holland. Space–time evolution of plasma instabilities-absolute and convective.

30. P. HUERRE 2000 In *Developments in Fluid Mechanics: A collection for the Millenium.* Cambdridge: Cambridge University Press. Open shear flow instability.

31. G. S. TRIANTAFYLLOU 1994 *Physics of Fluids* **6**, 164–171. Note on the Kelvin–Helmholtz instability of stratified fluids.

32. J. MIKLOWITZ 1978 *The Theory of Elastic Waves and Waveguides.* Amsterdam: North-Holland.

33. W. WEAVER, S. P. TIMOSHENKO and D. H. YOUNG 1990 *Vibration Problems in Engineering.* New York: John Wiley.

34. P. G. DRAZIN and W. H. REID 1981 *Hydrodynamic stability.* Cambridge: Cambridge University Press.

35. E. DE LANGRE 2001 in *IUTAM Symposium on Flow in Collapsible Tubes and Past Other Highly Compliant Boundaries, Warwick.* The effect of structural characteristics on the onset of absolute instability in compliant structures submitted to inviscid flow.